ADVANCES IN ATMOSPHERIC SCIENCES, VOL. 23, NO. 2, 2006, 190–198

A Comparison of the Radar Ray Path Equations and Approximations for Use in Radar Data Assimilation

Jidong GAO*[1], Keith BREWSTER[1], and Ming XUE[1,2]

[1] *Center for Analysis and Prediction of Storms, Sarkeys Energy Center, Norman, OK* 73019, *U.S.A*

[2] *School of Meteorology, University of Oklahoma, U.S.A*

(Received 6 April 2005; revised 15 June 2005)

ABSTRACT

The radar ray path equations are used to determine the physical location of each radar measurement. These equations are necessary for mapping radar data to computational grids for diagnosis, display and numerical weather prediction (NWP). They are also used to determine the forward operators for assimilation of radar data into forecast models. In this paper, a stepwise ray tracing method is developed. The influence of the atmospheric refractive index on the ray path equations at different locations related to an intense cold front is examined against the ray path derived from the new tracing method. It is shown that the radar ray path is not very sensitive to sharp vertical gradients of refractive index caused by the strong temperature inversion and large moisture gradient in this case. In the paper, the errors caused by using the simplified straight ray path equations are also examined. It is found that there will be significant errors in the physical location of radar measurements if the earth's curvature is not considered, especially at lower elevation angles. A reduced form of the equation for beam height calculation is derived using Taylor series expansion. It is computationally more efficient and also avoids the need to use double precision variables to mitigate the small difference between two large terms in the original form. The accuracy of this reduced form is found to be sufficient for modeling use.

Key words: Doppler radar, ray path equations, refractivity index, data assimilation

doi: 10.1007/s00376-006-0190-3

1. Introduction

The operational Doppler NEXRAD (WSR-88D) radar network is becoming more and more important in improving the real time detection and warning of hazardous weather (Alberty et al., 1991; Crum et al., 1998; Serafin and Wilson, 2000). It is viewed as an essential observing system for initializing non-hydrostatic, storm-resolving (i.e., horizontal grid spacing of order 1 km) numerical weather prediction (NWP) models (e.g., Lilly, 1990; Droegemeier, 1990, 1997). Attempts to demonstrate such capability began early in the past decade (e.g., Sun et al., 1991), and subsequent efforts have been notably successful (e.g., Gao et al., 1998; Weygandt et al., 2002a, b; Crook and Sun, 2002; Xue et al., 2003; Brewster, 2003; Gao et al., 2004).

To assimilate the radar reflectivity and radial velocity data from weather radar into an NWP model, it is necessary to use suitable ray path equations to obtain the physical location of each radar measurement and to have accurate forward operators to convert model winds to radial velocity in the data assimilation schemes. Currently, there are several versions of ray path equations in the textbooks (e.g., Doviak and Zrnic, 1993). Most studies in radar data assimilation use very simple straight line ray path equations to model the forward operator that projects the 3D wind fields from the NWP model onto the radial direction (e.g., Gao et al., 1998; Shapiro et al., 2003; Weygandt et al., 2002a, b). This paper aims at estimating errors caused by using simplified ray path equations. In the next section, we will review the radar ray path equations in different forms with and without considering earth curvature under the assumption that the standard atmosphere is considered. In section 3, we first derive a new stepwise ray tracing method, and then we examine the validity of the ray path equations when

*E-mail: jdgao@ou.edu

the vertical gradients of the refractive index of air are significantly different from those of the standard atmosphere during a strong cold front outbreak. In sections 4 and 5, we analyze the error of the beam height and horizontal distance calculation when earth curvature is not considered. The error for local slope angle θ'_e of the ray path, which is important when projecting the three-dimensional wind field onto the radial direction, is analyzed in section 6. Finally, a summary and further discussion are given in section 7.

2. The ray path equations and some other operators

Under the assumption that temperature and humidity are horizontally homogeneous so that the refractivity is a function only of the height above ground, Doviak and Zrnić (1993) derived a formulation that expresses the ray path in terms of a path following a curve of a sphere of radius a_e:

$$a_e = \frac{a}{1 + a\left(\frac{dn}{dh}\right)} = k_e a \,, \tag{1}$$

where a is the earth's radius and k_e is a multiplier which is dependent on the vertical gradient of the refractive index of air, dn/dh. The refractive index of air, n, is a function of temperature, pressure and humidity and is usually taken, subject to certain assumptions, as (Beam and Dutton, 1968),

$$N = (n-1) \times 10^{-6} = 77.6P/T + 3.73 \times 10^{-5} eT^{-2} \,, \tag{2}$$

where P is air pressure in hPa (including water vapor pressure), e is water vapor pressure in hPa, and T is air temperature in K. It is convenient to use the quantity N, called the radio refractivity, instead of n. N represents the departure of n from unity in parts per million. N has a value of about 300 (at the surface) and its variations can be considered more conveniently. In the above equation, the first term on the right hand side is known as the dry term, and the second term is the moist term. The value of N can be computed from measurements of P, T, and e. When the Standard Atmosphere is considered, it is found that k_e is equal to 4/3 (Doviak and Zrnić, 1993). This is often referred to as the "four-thirds earth radius model". If N decreases more (less) rapidly with height than the Standard Atmosphere, the beam may be refracted more (less), and in such cases, the height of a target may be overestimated (underrestimated) by the four-thirds earth radius model. In an extreme condition (a sharp refractivity gradient of -300 N km^{-1} below 100 m in height), a ray sent at a positive elevation angle may actually decrease in height with range and eventually strike the earth (Doviak and Zrnić, 1993).

The following two equations relate h and the surface range (distance along the earth's surface), s, to radar-measurable parameters, the slant path, r, and radar elevation angle, θ_e (Doviak and Zrnić, 1993),

$$s = k_e a \sin^{-1}\left(\frac{r\cos\theta_e}{k_e a + h}\right) \,, \tag{3}$$

$$h = [r^2 + (k_e a)^2 + 2rk_e \sin\theta_e]^{1/2} - k_e a \,. \tag{4}$$

To derive an expression relating the radial velocity, which is measured by the radar, to the wind at the measurement point (r, θ_e, ϕ), where ϕ is the azimuth angle, a combined spherical and Cartesian coordinate system is used with x and y as the arc distances from the radar along two orthogonal great circle paths. We choose y to be along a longitude, with north as the positive direction. z measures the height above the antenna height of the beam. The horizontal components u and v of the vector wind $\boldsymbol{v}$ are tangent to the great circle arcs at x and y, respectively, and are directed eastward. The vertical component w of $\boldsymbol{v}$ is along z, with $z = 0$ at the height of the radar feedhorn. Some of the symbols used in Eqs. (3)–(11) are listed in Table 1.

Table 1. List of symbols for Eqs.(3)–(11)

Symbol	Description
s	Surface range of ray path using standard ray path Eq. (3)
h	Beam height
x, y, z	Cartesian coordinates for curved ray path when the earth curvature is considered
θ	Radar elevation angle
θ'_e	Angle between the radar beam and the tangent plane below the data point
s'	Surface range of ray path using approximation (7)
v_r	Radial velocity for the curved ray path
x^*, y^*, z^*	Cartesian coordinates for straight line ray path when the earth curvature is not considered
v_r^*	Radial velocity for the straight line ray path
s^*	Surface range for the straight line ray path

In their textbook, Doviak and Zrnić (1993) also show that if $r \ll k_e a$, the coordinates x, y and z are related to the radar coordinates (r, θ_e, ϕ) by,

$$x \approx r \cos\theta'_e \sin\phi \,, \tag{5a}$$

$$y \approx r \cos\theta'_e \cos\phi \,, \tag{5b}$$

$$z = h = (k_e a + r^2 + 2 r k_e a \sin\theta'_e)^{1/2} - k_e a \,, \tag{5c}$$

where θ'_e, the angle between the radar beam and the tangent plane below the data point, is the sum of two terms expressed as the following (Brewster, 2003),

$$\theta'_e = \theta_e + \tan^{-1}[r\cos\theta_e/(k_e a + r\sin\theta_e)] \,. \tag{6}$$

From Eqs. (5a) and (5b), one can easily derive the distance along the earth's surface as,

$$s' \approx r \cos\theta'_e \,. \tag{7}$$

The radial velocity v_r is the projection of $\boldsymbol{v}$ onto $\boldsymbol{r}$, the vector from the radar to the point (r, θ_e, ϕ). Again, if $r \ll k_e a$,

$$v_r = u\cos\theta'_e \sin\phi + v\cos\theta'_e \cos\phi + (w - w_t)\sin\theta'_e \,. \tag{8}$$

For some applications, where $r \ll k_e a$, previously published NWP research has typically ignored the influence of earth curvature and further reduced the above equations, treating the radar ray path as a straight line over a flat earth. In such a case, Eqs. (5), (7), and (8) are simplified as,

$$x^* \approx r\cos\theta_e \sin\phi \,, \tag{9a}$$

$$y^* \approx r\cos\theta_e \cos\phi \,, \tag{9b}$$

$$z^* \approx r\sin\theta_e \,, \tag{9c}$$

$$v_r^* = u\cos\theta_e \sin\phi + v\cos\theta_e \cos\phi + (w - w_t)\sin\theta_e \,, \tag{10}$$

$$s^* \approx r\cos\theta_e \tag{11}$$

Equations (7) and (11) are two different forms of approximation of ray path equation (3). Equation (5c) uses exactly the four-thirds earth beam height equation (4), and (9c) is an approximation of (4). In the following sections, we will first examine the influence of refractive index on the ray path equations based on a stepwise ray trace method, then we will investigate whether the simplified ray path equations are appropriate.

3. Influence of refractive index

Typically, the four-thirds earth radius model has been used for radar ray paths, assuming the refractivity index is linearly dependent on height in the first kilometer of the atmosphere. However, the gradient of the refractive index is not always a constant, and departures from linearity may exist when there are strong temperature inversions or large moisture gradients with height. In the following study, we will examine the influence of several different environmental thermodynamic profiles on the radar ray path. To accurately estimate the radar ray path, we develop a stepwise ray tracing method as follows:

(1) Starting from the first gate near the radar location, for each radar measurement, calculate the refractivity N_{i-1} for the previous gate according to Eq. (2) using different thermodynamic profiles and gradients of refractive index according to the differential of Eq. (2) with respect to beam height,

$$\left.\frac{dn}{dh}\right|_{i-1} = 10^6 \left.\frac{dN}{dh}\right|_{i-1} \tag{12}$$

Here i is the index of the gate.

(2) Calculate $a_{e,i-1} = k_{e,i-1} a$ according to Eq. (1) using the gradient of refractive index from step (a) at each gate.

(3) Calculate the angle between the radar beam and the tangent plane below the data point, $\theta'_{e,i-1}$ using Eq. (6) for each radar beam gate.

(4) Finally, the radar beam height h and the surface range s can be calculated using the following formulation,

$$\begin{cases} h_i = h_{i-1} + \Delta r \times \sin\theta'_{e,i-1} \,, \\ s_i = s_{i-1} + \Delta r \times \cos\theta'_{e,i-1} \,, \end{cases} \tag{13}$$

where Δr is gate spacing, with 250 m for NEXRAD radial winds. Variables h_i and s_i are the beam height and surface distance for each gate, respectively. Steps (1) through (4) are repeated from the first (i=1) until the last gate of the radar measurement.

As an example, we apply the above procedure to an intense cold front outbreak in the Southern Plains of the United States in the winter of 1990 documented in the textbook of Bluestein (1993). Figure 1 shows four different temperature and dew point profiles within the Southern Plains at 1200 UTC 21 December 1990. At this time, a surface analysis indicates an intense cold front along the boundary of Oklahoma and Arkansas, and the eastern part of Texas. Two of the profiles (Figs. 1a, 1b), Lake Charles, Louisiana (LCH) and Longview, Texas (GGG) are on the warm side of the front; the other two stations, Norman, Oklahoma (OUN) and North Platte, Nebraska (LBF) are on the cold side of the front (Figs. 1c, 1d). The air in the frontal zone is humid on both sides of the front; and the air above the frontal zone is relatively warm and dry. At the Norman and North Platte sites, there is a pronounced frontal inversion between 900 and 850 hPa. The profiles of vertical radio refractivity gradient are shown in Fig. 2. It might be expected that there exist large refractivity gradients between 900 and 850 hPa

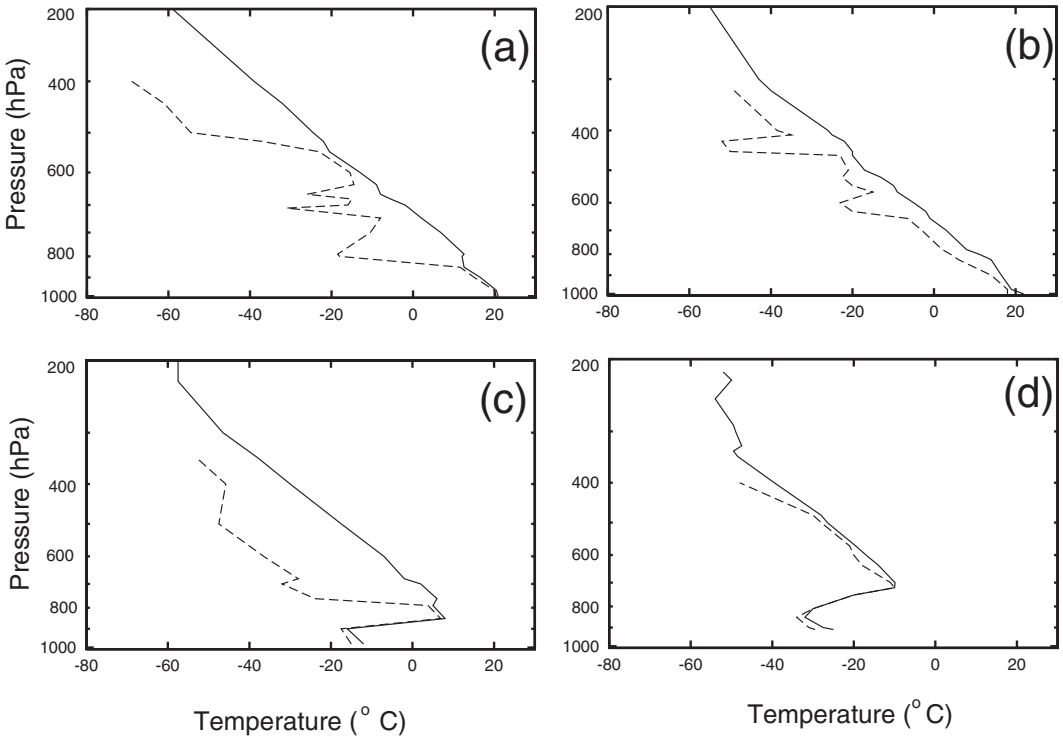

Fig. 1. The temperature (solid) and dew point (dashed) profiles for 1200 UTC 21 December 1990, at (a) Lake Charles, Louisiana (LCH), (b) Longview, Texas (GGG), (c) Norman, Oklahoma (OUN), and (d) North Platte, Nebraska (LBF), abscissa is temperature (°C); ordinate is pressure (hPa).

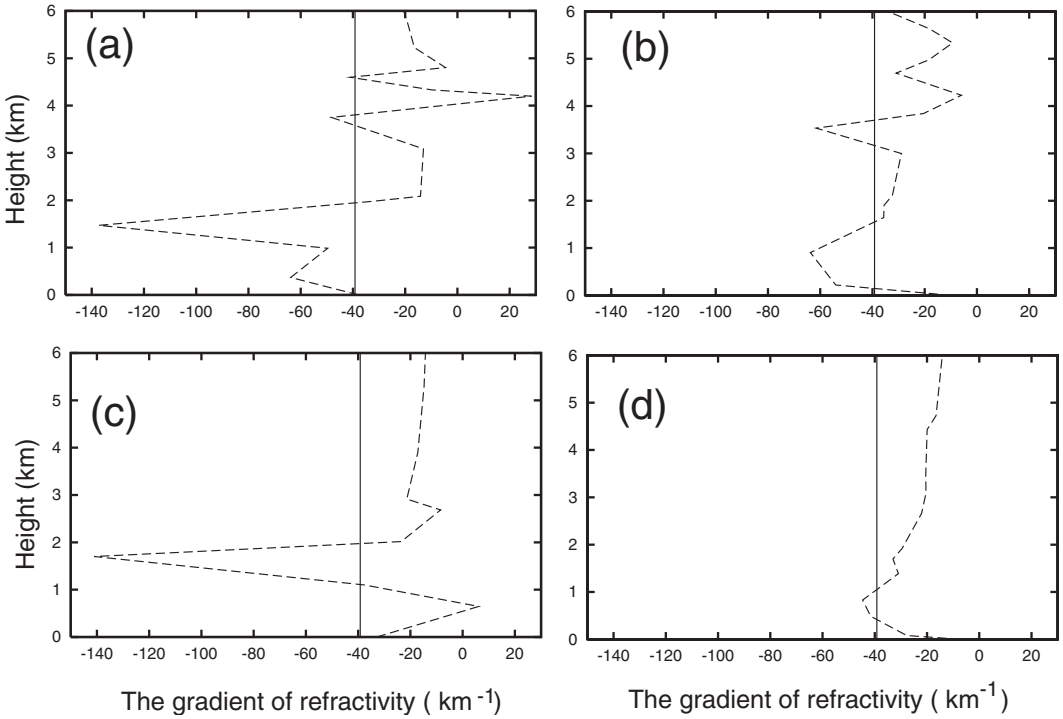

Fig. 2. The refractivity gradient profiles (km^{-1}) for 1200 UTC 21 December 1990, at (a) Lake Charles, Louisiana (LCH), (b) Longview, Texas (GGG), (c) Norman, Oklahoma (OUN), and (d) North Platte, Nebraska (LBF). The solid line is the refractivity gradient for the standard atmosphere; the dashed lines represent observed conditions.

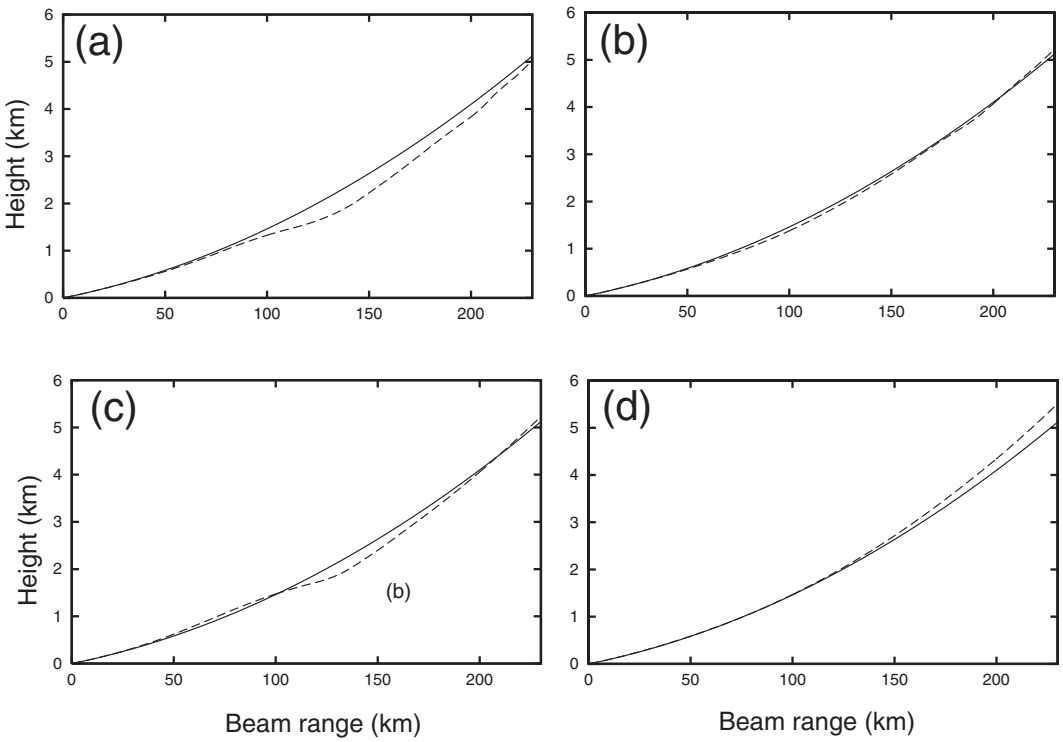

Fig. 3. The radar ray paths calculated for 0.5° elevation angle using the refractivity gradients derived from (a) Lake Charles, Louisiana (LCH), (b) Longview, Texas (GGG), (c) Norman, Oklahoma (OUN), and (d) North Platte, Nebraska (LBF) using the stepwise method (dashed lines), as compared to those derived from the standard atmosphere refractivity gradient (solid lines).

because of the strong temperature inversion and sharp moisture gradients at the Norman and Lake Charles sites (Figs. 2a and 2c). However, the gradients of refractivity are close to normal for the North Platte site, which only has a strong temperature inversion, while the other soundings exhibit large deviations from the standard atmosphere at levels with strong moisture gradients. So it is seen that the gradients of radio refractivity are fairly sensitive to vertical variations in humidity. To quantitatively estimate such sensitivity is very difficult because the refractivity gradient is a complicated function of humidity.

Figure 3 shows the variations of radar beam height with the range gate for a 0.5° elevation angle. The solid line is the ray path calculated from Eqs. (3) and (4) with the standard atmosphere condition and the dashed line is the ray path calculated using the stepwise method with the refractivity gradients derived from the observed thermodynamic profiles. It is shown that for all four soundings, the calculated beam heights are generally close to the ray paths that are derived from the standard atmospheric condition, with some small variations, despite strong departure from the standard atmosphere in some layers. One can see that for the Lake Charles and Norman sites (Figs. 3a and 3c), the radar beam is refracted downward toward the earth surface due to the sharp refractivity gradient near the 1.5 km level. The largest difference in the beam height is about 400 m and occurs with the Lake Charles sounding at about 1.5 km in height. The relative error with respect to beam width is about 17%. For Longview and North Platte, the calculated ray path is very close to that for the standard atmospheric condition. For the higher elevation angles, the radar ray paths are even less sensitive to the refractivity gradients (not shown). Suppose that the error for beam height relative to beam width should be no more than 50%, then we can see that for this case which had profiles typical of a strong cold front, with strong temperature inversion and vertical moisture gradient, that the use of the four-thirds earth radius model predicts beam height with sufficient accuracy for numerical modeling using weather radar data. In Doviak and Zrnić (1992), it is stated that for weather radar applications, the four-thirds earth radius model can be used for all ray paths if beam height, h, is restricted to the first 10–20 km and if refractive index, n, has a gradient of about $-1/4a$ in the first kilometer of the atmosphere. It is still true for this extreme case that refractive index has gradients that are significantly less

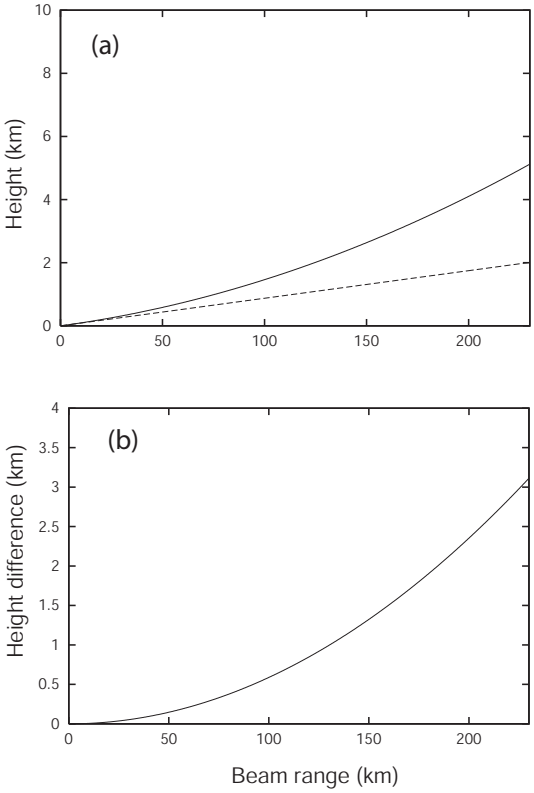

Fig. 4. (a) The variations of radar beam height with the range gate for elevation angle 0.5°. The solid line is calculated by the four-thirds earth ray path Eq. (5c), and the dashed line is calculated by the straight line ray path approximation Eq. (9c); (b) The absolute difference in beam height calculated from the two formulas given by Eq. (5c) and Eq. (9c).

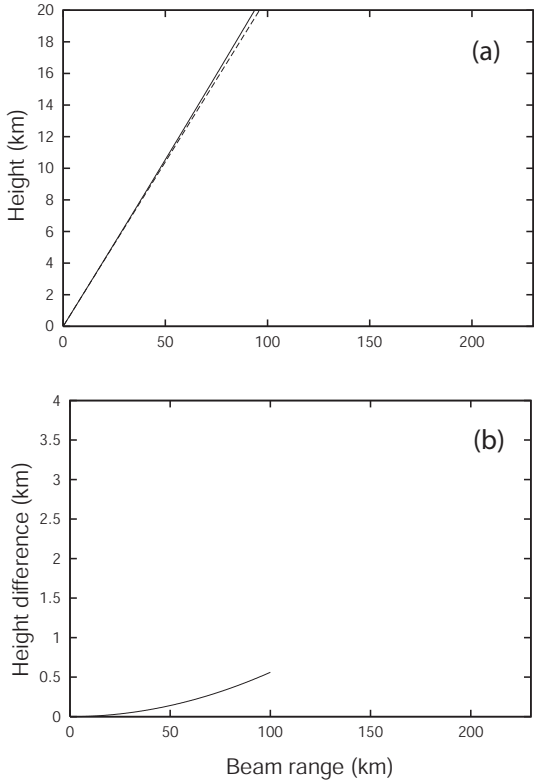

Fig. 5. As in Fig. 4, but for the case when elevation angle is 12°. Beam heights greater than 20 km are not shown because typically there is no weather signal above the 20-km level.

than $-1/4a$ at some levels.

Certainly there exist cases where ducting and strong departures from the four-thirds earth radius model can and do occur. We are using the above procedure (12)–(13) to verify the beam path equation (3) and (4) under a range of locations across the United States for several decades to quantify the relative occurrence of significant departures. This climatological study will be published separately.

4. Error analysis of the beam height calculation

Because the total number of radar data to be used in a data assimilation application can be quite voluminous, it would be practical to use the simplified equations for the beam path to improve computational efficiency. Simplified equations are also used in the literature at times to improve tractability. In this section, we discuss the errors of beam height calculation using the simplified Eq. (9c) as compared to Eq. (4). To examine the errors for the lower elevation angle, we first choose elevation $\theta_e = 0.5°$ and ranges from 0 to 230 km with a range resolution of 250 m. Figure 4a shows the comparison of radar beam heights calculated by Eqs. (4) and (9c), while Fig. 4b shows the absolute differences in beam heights calculated using these two formulas. One can see that the two curves stay relatively close to each other only for ranges less than 30 km. At the 30-km range, the error is about 50 m; at 100 km, the error reaches 500 m. At 230 km, the error grows to 3112 m. This demonstrates that it may not be appropriate to use Eq. (9c) to calculate the beam height for low elevation angles. When the elevation angle θ_e is increased to 12°, it is shown that the two beam height curves remain within 500 m of each other until the range of 100 km (Fig. 5a). Although the relative error is small, the absolute difference between the two estimates is nearly the same as that of the low elevation angle case. Figure 6 shows the relative errors with respect to radar beam width, calculated using Eq. (9c) instead of the four-thirds earth ray path equation Eq. (4). It is shown that for both elevation angles of 0.5° and 12°, the relative errors are quite large for most of the gates. Though at a range of 30 km, the relative error is only about 10%; as the beam reaches 230 km,

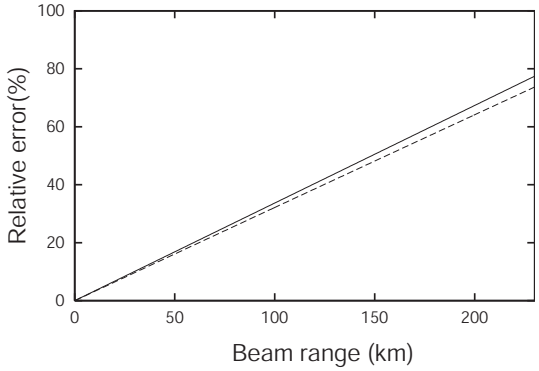

Fig. 6. The relative errors of beam height to radar beam width calculated by the straight line path approximation (9c). The solid line is for elevation angle 0.5° while the dashed line is for 12°.

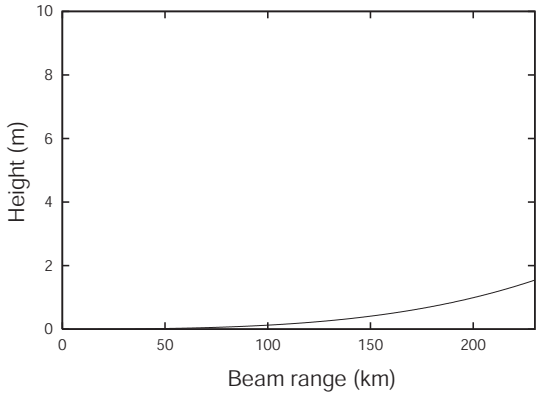

Fig. 7. The difference between the beam heights given by approximate formula (12) and true beam path equation (2) for elevation angle 0.5°.

the relative errors exceed 70%. So for most applications, it is necessary to use the curved ray path equation (4) to calculate the height of the radar measurement locations, instead of the simplified Eq. (9c).

However, numerically evaluating the beam height of each radar measurement using the original formula, Eq. (4), is complicated and double precision is usually required because the right hand side of Eq. (4) is a small difference between two large terms. A possible reduction of Eq. (4) for computational efficiency is examined in the following.

Rearranging Eq. (4) yields,

$$h = k_e a(1+x)^{1/2}\,, \tag{14}$$

where,

$$x = \frac{r^2 + 2rk_e a\sin\theta_e}{(k_e a)^2}\,. \tag{15}$$

Obviously, $x \ll 1$, using Taylor series expansion and in keeping the first order, h can be expressed as,

$$h \approx r\sin\theta_e + \frac{r^2}{2k_e a}\,. \tag{16}$$

This equation is a much better approximation than Eq. (5c). Figure 7 shows the difference between the beam heights given by (4) and (14) as a function of beam range for elevation angle 0.5°. The maximum difference at range 230 km is only about 1.5 m. Equation (16), a much simplified form, is therefore a good approximation to Eq. (4) and suitable for use when efficiency is important and many calculations must be done.

5. The surface range (distance along the earth's surface)

In last section, we performed error analyses for beam height. In this section, we will estimate whether the calculation for the horizontal location of each radar measurement using the reduced Eqs. (9a) and (9b) give good approximations to Eqs. (5a) and (5b). To do that, we only need to determine if Eqs. (7) and (11) are good approximations to ray path Eq. (3). Figure 8a shows absolute errors of Eqs. (7) and (11), that is, the variations of $|s' - s|$ and $|s^* - s|$ as a function of range at low elevation angle 0.5°. One can see that Eq. (7) gives an excellent estimate of surface range as compared to Eq. (3). But Eq. (11) gives a good estimate only for radar measurements less than 100 km. When the radar elevation angle is 12°, one can see that the errors for surface range calculated using both Eqs. (7) and (11) are larger, but Eq. (7) still gives a very good estimate of the surface range (Fig. 8b), as even at distant ranges, the difference is less than a single range gate. Equation (11) introduces some error, but it can still be used because, for this elevation angle, the radar ray is at a height above 10 km at 50 km range (note that at 50 km range, the horizontal position error is about 60 m, about one quarter of the range resolution of the NEXRAD). So we can conclude that for determining the horizontal location of the radar measurement, Eq. (7) is a very good approximation, and Eq. (11) may also be acceptable for ranges less than 50 km.

6. Local slope angle θ'_e of the Ray Path

Equation (6) describes the calculation of the local slope angle of the radar beam, θ'_e, which is the angle between the radar beam and the earth's tangent plane below the data point. This is an important variable because we use it not only to calculate the location of the radar measurement, but also to calculate the radial velocity in the forward operator within radar data assimilation, as in Eq. (8). Figure 9 shows the variation of local slope angle, θ'_e, with the range. For

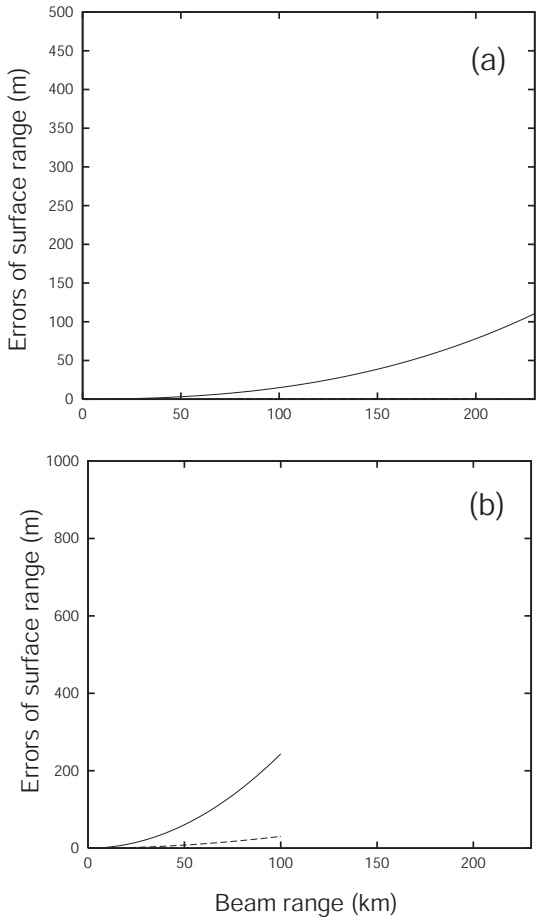

Fig. 8. (a) The differences in surface ranges given by the true ray path equation and its two forms of approximation at elevation angle 0.5°. The dashed line is for the curved ray path formula (7) and the solid line is for the straight line ray path formula (11). (b) The same as (a), but for elevation angle 12°. Note that the dashed line in (a) superposes the horizontal axis.

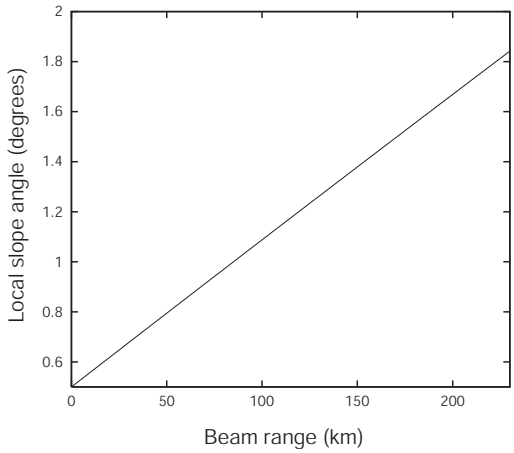

Fig. 9. The variation of local slope angle as a function of beam range for elevation angle 0.5°.

a low elevation of 0.5°, θ'_e increases with range, becoming 1.84° at 230 km, almost 4 times the original elevation angle at the radar antenna; while for a higher elevation of 12°, θ'_e reaches 13.33° at the range of 230 km (not shown). So the relative changes of local slopes are more significant for lower elevation angles than for high elevation angles.

Suppose that at one radar gate, we have a horizontal wind $u = v$ =30 m s^{-1}, a vertical velocity w=15 m s^{-1} and a terminal fall velocity w_t=5 m s^{-1}, with the azimuthal angle being $\phi = 45°$. Substitute these values into Eq. (10), and we get V_r=42.51 m s^{-1} for elevation angle 0.5° and V_r=42.73 m s^{-1} for elevation angle 1.84°. So the difference in radial velocity is only 0.22 m s^{-1}, much less than the expected error of the measurement itself, even though the local elevation angles vary by a factor of 4 (see Fig. 9). Since the NEXRAD radar usually operates at relatively low elevation angles (generally below 20°), and since $\sin\theta'_e$ is small compared to other terms on the left hand side of the forward operators (8) and (10), the contribution of vertical velocities and terminal fall velocities to radial velocities remains relatively small. The variation of $\cos\theta'_e$ is also not very sensitive to θ'_e with the increase of range gate for a fixed elevation angle; this leads to Eq. (10) being an acceptable approximation to Eq. (8).

7. Summary and discussion

The radar ray path equations are needed to determine the forward operators for the assimilation of radar data into forecast models. In this paper, we review the ray path equations in several forms and develop a new stepwise ray tracing method. The influence of the atmospheric refractive index to the ray path equations at different locations related to an intense cold front is examined. It is shown that the radar ray path is not very sensitive to the relatively large vertical gradients of refractive index caused by the large temperature inversion and moisture gradients in this intense cold front environment.

In some published works, radar ray paths have been approximated as straight lines. This simplifies the equations used to determine the physical location of each radar measurement, but introduces errors that are significant for ranges beyond 30 km. It is found that the calculation of the physical location of each radar measurement may have significant error if the four-thirds earth ray path equations are not used, especially when the radar is operated at low elevation angles. A reduced form of the equation for beam height is derived in this paper using Taylor series expansion, which is computationally more efficient and also avoids the need to use double precision variables to mitigate

the small difference between two large terms in the original form. This form is found to be rather accurate.

It is demonstrated that for the horizontal location of the radar measurement, Eq. (7) is a very good estimate, and Eq. (11) can also be acceptable for radar measurements within the 50-km range. We also find that the radial velocity forward operator that projects the three components of wind onto the radial direction under the assumption of straight-line ray paths gives a reasonable approximation under typical operating conditions. The results of this paper provide useful guidances to radar data analysis and assimilation applications in which both efficiency and accuracy are important.

Acknowledgments. This work was supported by US NSF ATM-0129892, ATM-0331756, ATM-0331594 and EEC-0313747, and DOT-FAA grant NA17RJ1227-01. The first author was also partly supported by the National Natural Science Foundation of China for young investigators (Grant No. 40505022). Ming Xue was also supported by the Outstanding Overseas Scholars Award of the Chinese Academy of Sciences (Grant No. 2004-2-7). Graphic plots were generated by the GNUPLOT graphics package.

REFERENCES

Alberty, R. L., T. D. Crum, and F. Toepfer, 1991: The NEXRAD program: Past, present, and future–A 1991 perspective. Preprints, *25th Int. Conf. on Radar Meteorology*, Paris, Amer. Meteor. Soc., 1–8.

Bean, B. R., and E. J. Dutton, 1968: *Radio Meteorology.* Dover Publications, 435pp.

Brewster, K. A., 2003: Phase-correcting data assimilation and application to storm scale numerical weather prediction. Part II: Application to a severe storm outbreak. *Mon. Wea. Rev.*, **131**, 493–507.

Bluestein, H. B., 1993: *Synoptic-Dynamic Meteorology in Midlatitudes.* Volume II, Oxford University Press, Inc, 594pp.

Crook, N. A., and J. Sun, 2002: Assimilating radar, surface, and profiler data for the Sydney 2000 Forecast Demonstration Project. *J. Atmos. Oceanic Technol.*, **19**, 888–898.

Crum, T. D., R. E. Saffle, and J. W. Wilson, 1998: An update on the NEXRAD Program and future WSR-88D support to operations. *Wea. Forecasting*, **13**, 253–262.

Doviak, R. J., and D. S. Zrnić, 1993: *Doppler Radar and Weather Observations.* Academic Press, 2nd ed., 562pp.

Droegemeier, K. K., 1990: Toward a science of storm-scale prediction. Preprint, *16th Conf. on Severe Local Storms*, Kananaskis Park, Alberta, Canada, Amer. Meteor. Soc., 256–262.

Droegemeier, K. K., 1997: The numerical prediction of thunderstorms: Challenges, potential benefits, and results from real time operational tests. *WMO Bulletin*, **46**, 324–336.

Gao, J., M. Xue, Z. Wang, and K. K. Droegemeier, 1998: The initial condition and explicit prediction of convection using ARPS forward assimilation and adjoint methods with WSR-88D data. Preprints, *12th Conference on Numerical Weather Prediction*, Phoenix, AZ, Amer. Meteor. Soc., 176–178.

Gao, J., M. Xue, K. Brewster, and K. K. Droegemeier 2004: A three-dimensional variational data assimilation method with recursive filter for single-Doppler radar. *J. Atmos. Oceanic Technol.*, **21**, 457–469.

Lilly, D. K., 1990: Numerical prediction of thunderstorms—Has its time come? *Quart. J. Roy. Meteor. Soc.*, **116**, 779–798.

Serafin, R. J., and J. W. Wilson, 2000: Operational weather radar in the United States: Progress and opportunity. *Bull. Amer. Meteor. Soc.*, **81**, 501–518.

Shapiro, A., P. Robinson, J. Wurman, and J. Gao, 2003: Single-Doppler velocity retrieval with rapid-scan radar data. *J. Atmos. Oceanic Technol.*, **20**, 1758–1775.

Sun, J., D. W. Flicker, and D. K. Lilly, 1991: Recovery of three-dimensional wind and temperature fields from simulated single-Doppler radar data. *J. Atmos. Sci.,* **48**, 876–890.

Sun, J., and N. A. Crook, 2001: Real-time low-level wind and temperature analysis using single WSR-88D data. *Wea. Forecasting*, **16**, 117–132.

Weygandt, S. S., A. Shapiro, and K. K. Droegemeier, 2002a: Retrieval of initial forecast fields from single-Doppler observations of a supercell thunderstorm. Part I: Single-Doppler velocity retrieval. *Mon. Wea. Rev.*, **130**, 433–453.

Weygandt, S. S., A. Shapiro, and K. K. Droegemeier, 2002b: Retrieval of initial forecast fields from single-Doppler observations of a supercell thunderstorm. Part II: Thermodynamic retrieval and numerical prediction. *Mon. Wea. Rev.*, **130**, 454–476.

Xue, M., D.-H. Wang, J. Gao, K. Brewster, and K. K. Droegemeier, 2003: The Advanced Regional Prediction System (ARPS), storm-scale numerical weather prediction and data assimilation. *Meteorology and Atmospheric Physics*, **82**, 139–170.